T2-adjusted computed diffusion-weighted imaging: a novel method to enhance tumour visualization

Lin Cheng*[1], Matthew D Blackledge*[†1], David J Collins[1], Matthew R Orton[1], Neil P Jerome[1], Thorsten Feiweier[2], Mihaela Rata[1], Veronica Morgan[3], Nina Tunariu[1,3], Martin O Leach[1], and Dow-Mu Koh[1,3]

1. Cancer Research UK Cancer Imaging Centre, Division of Radiotherapy and Imaging, The Institute of Cancer Research, London, UK
2. Siemens Healthcare GmbH, Erlangen, Germany
3. Department of Radiology, Royal Marsden Hospital, Sutton, UK

*L Cheng and M D Blackledge have made equal contributions to this text.
† Correspondence: Dr. Matthew Blackledge, Cancer Research UK Cancer Imaging Centre, Division of Radiotherapy and Imaging, The Institute of Cancer Research, London, UK E-mail: matthew.blackledge@icr.ac.uk

Abstract

Purpose

To introduce T_2-adjusted computed DWI (T_2-cDWI), a method that provides synthetic images at arbitrary b-values and echo times (TEs) that improve tissue contrast by removing or increasing T_2 contrast in diffusion-weighted images.

Materials and Methods

In addition to the standard DWI acquisition protocol T_2-weighted echo-planar images at multiple (≥2) echo times were acquired. This allows voxelwise estimation of apparent diffusion coefficient (ADC) and T_2 values, permitting synthetic images to be generated at any chosen b-value and echo time. An analytical model is derived for the noise properties in T_2-cDWI, and validated using a diffusion test-object. Furthermore, we present T_2-cDWI in two example clinical case studies: (i) a patient with mesothelioma demonstrating multiple disease tissue compartments and (ii) a patient with primary ovarian cancer demonstrating solid and cystic disease compartments.

Results

Measured image noise in T_2-cDWI from phantom experiments conformed to the analytical model and demonstrated that T_2-cDWI at high computed b-value/TE combinations achieves lower noise compared with conventional DWI. In patients, T_2-cDWI with low b-value and long TE enhanced fluid signal while suppressing solid tumour components. Conversely, large b-values and short TEs overcome T_2 shine-

through effects and increase the contrast between tumour and fluid compared with conventional high-b-value DW images.

Conclusion

T_2-cDWI is a promising clinical tool for improving image signal-to-noise, image contrast, and tumour detection through suppression of T_2 shine-through effects.

Key words:

Diffusion-weighted imaging, computed DWI, tumour enhancement, T2 contrast, T2 shine-through effect.

Introduction

Diffusion-weighted magnetic resonance imaging (DWI) is a non-invasive functional imaging technique, where endogenous image contrast is generated through differences in the rate of diffusion of water molecules in different environments. DWI is particularly attractive in oncological applications as the rate of extracellular water diffusion is thought to provide a surrogate marker of tissue cellularity and the integrity of cell membranes[1-3]. In recent years, DWI has become mandatory as a source of oncological imaging biomarkers for tumour detection and characterization [1]. Furthermore, it has shown great promise for the assessment of early treatment response due to its ability to non-invasively provide quantitative and qualitative information at the cellular level throughout the course of therapy[4; 5].

Computed diffusion-weighted imaging (cDWI) has previously been proposed for achieving improved image contrast and signal-to-noise ratio (SNR) through the synthesis of images with arbitrary 'diffusion weighting' (b-value); by acquiring images at a range of lower b-values, it is possible to generate synthetic images corresponding to arbitrarily high b-values without increasing the scan acquisition time[6]. However, as cDWI is intrinsically T_2-weighted it is often unable to distinguish between cellular disease and tissues with long T_2-relaxation times (e.g. cystic areas, necrosis, fluid, pleural effusion), leading to a diagnostic misinterpretation phenomenon known as `T_2 shine-through'.

In this study we propose a novel method, T_2-adjusted computed diffusion-weighted imaging (T_2-cDWI), to produce both ADC and T_2, thus enabling the generation of synthetic images corresponding to both arbitrary b-value and echo time (TE) by

acquiring a small subset of additional images with different (≥2) echo times. This implementation allows clinicians to independently modify the level of diffusion- and T_2-weighting for a given image and retrospectively remove or isolate the T_2-shine-through effect [7].

In this article we describe the technology required to perform this novel imaging strategy, derive mathematical approximations for the noise in T_2-cDWI, and validate these models using a diffusion test-object. We further present two clinical examples of T_2-cDWI where adjusting the T_2 and/or diffusion contrast provides improved clinical interpretation of disease.

Materials and Methods

T_2-cDWI Model

We utilise a spin-echo echo-planar imaging (SE-EPI) sequence that allows for the acquisition of images at multiple combinations of b-values and echo times. The intensity for a given pixel location in the magnitude image may be modelled by:

$$S_i(b_i, TE_i) = S_0 \cdot \exp\{-b_i \cdot ADC\} \cdot \exp\{-TE_i \cdot R_2\} + \varepsilon_i \quad (1)$$

for the *i*th combination of b and TE, where ADC and $R_2 = 1/T_2$ are the tissue apparent diffusion coefficient and transverse relaxivity respectively. We assume $\varepsilon_i \sim N(0, \sigma_i)$ to be the additive noise. T_2-cDWI is an approach whereby enough combinations of b and TE are acquired (at least 3) such that ADC and R_2 may be estimated and then used to generate signal contrast at b_c and TE_c, the desired b-value and TE:

$$S_c(b_c, TE_c) = \widehat{S_0} \cdot \exp\left\{-b_c \cdot \widehat{ADC}\right\} \cdot \exp\left\{-TE_c \cdot \widehat{R_2}\right\} \quad (2)$$

where $\widehat{S_0}, \widehat{ADC}, \widehat{R_2}$ are the corresponding estimated values for each voxel determined from the joint fitting.

Noise considerations for T_2-cDWI

Equation 1 may be considered a special case of a family of exponential functions:

$$\underline{S} = \exp\left\{\underline{\underline{X}} \cdot \underline{\alpha}\right\}, \qquad \underline{\underline{X}} = \begin{pmatrix} b_1 & TE_1 & 1 \\ \vdots & \vdots & \vdots \\ b_N & TE_N & 1 \end{pmatrix}, \qquad \underline{\alpha} = \begin{pmatrix} ADC \\ R_2 \\ \ln S_0 \end{pmatrix}$$

such that linearized least-squares estimate of the tissue parameters is given by:

$$\underline{\hat{\alpha}} = \left(\underline{\underline{X}}^{\mathrm{T}}\underline{\underline{X}}\right)^{-1}\underline{\underline{X}}^{\mathrm{T}} \ln \underline{S}$$

In matrix notation we may write equation 2 as

$$S_c = \exp\left\{\underline{\underline{X}}_c \cdot \underline{\hat{\alpha}}\right\} = \exp\{A \cdot \ln \underline{S}\} = \prod_{i=1}^{N} S_i^{A_i}, \quad \mathrm{X}_c = (b_c, TE_c, 1) \qquad (3)$$

$$\text{where} \quad \underline{A} = \underline{\underline{X_c}} \cdot \left(\underline{\underline{X}}^T\underline{\underline{X}}\right)^{-1}\underline{\underline{X}}^T$$

Using error propagation it is possible to approximate the expected variance of S_c:

$$\sigma_c^2 \approx S_c^2 \cdot \sum_{i=1}^{N}\left(\frac{A_i}{S_i}\right)^2 \sigma_i^2 \qquad (4)$$

The N-vector **$\underline{\mathbf{A}}$**, which depends only on the acquisition parameters of the scan and the desired computed b-values and TEs, can be complex to compute in the general case. We suggest an optimised imaging protocol for calculations of ADC and R_2 according to the methodology proposed in [8; 9]: For every image acquired at a minimum possible b-value and echo time (b_1=0, TE_1=TE_m) for the scanner, 3 images should be acquired with (b_2=0, TE_2=TE_m+ΔTE_{opt}) , and 3 images acquired with (b_3=b_{opt}, TE_3). The values are optimised according to the expected tissue properties: $b_{opt} \approx 1.28/ADC$ (ignoring the effects of b-value dependence on minimum echo time [10]), $\Delta TE_{opt} \approx 1.28/R_2$ [8; 11].

TE_3 should be the minimum echo time achievable on the scanner for the high b-value acquisition (for our protocol and scanners a lookup table has been derived to provide the minimum TE over the range $0 \leq b \leq 6000 s/mm^2$, although approximations are available in [11]). For this specially optimised protocol we find that:

$$\underline{A} = \left(-\frac{b_c(TE_2 - TE_3)}{b_3(TE_2 - TE_1)} - \frac{(TE_c - TE_2)}{(TE_2 - TE_1)}, -\frac{b_c(TE_3 - TE_1)}{b_3(TE_2 - TE_1)} - \frac{(TE_1 - TE_c)}{(TE_2 - TE_1)}, \frac{b_c}{b_3} \right)$$

$$S_c = S_1^{A_1} \cdot S_2^{A_2} \cdot S_3^{A_3} \quad (5)$$

$$\sigma_c^2 \approx \sigma^2 e^{-2b_c ADC} e^{-2TE_c R_2} \left\{ \frac{A_1^2}{e^{-2TE_1 R_2}} + \frac{A_2^2}{3e^{-2TE_2 R_2}} + \frac{A_3^2}{3e^{-2TE_1 R_2} e^{-2b_3 ADC}} \right\} \quad (6)$$

where σ^2 is the noise variance for the image acquired with one signal average.

It may be noted that for this protocol multiples of 7 image acquisitions are required to perform the T_2-cDWI calculation. It is therefore of interest to consider regions where $\sigma_c^2 < \sigma^2/7$, where improvements in noise may be gained using T_2-cDWI over conventionally acquired data. Figure 1 demonstrates the theoretical advantages in noise can be achieved using this suggested T2-cDWI protocol for a wide range of desired b_c and TE_c. Furthermore, T_2-cDWI allows the generation of contrast in regions where it would not be possible to directly acquire the data (i.e. where $TE_c < TE_{min}(b_c)$).

Validation of T2-cDWI models using a diffusion test-object

We validate equation (6) using a diffusion test-object consisting of 5 vials containing sucrose, manganese chloride and water with differing ADC ($0.7\text{-}1.1 \times 10^{-3} mm^2/s$) and T_2 (75-1408ms) properties at 0°C (Figure 2).

Three axial images were acquired at the isocenter of a 1.5T system (MAGNETOM Avanto, Siemens Healthcare, Erlangen, Germany) using a prototype monopolar, SE-EPI sequence with the following parameters: b-value=0/0/1100s/mm² (three optimized orthogonal

diffusion directions (three optimized, orthogonal diffusion directions (3-Scan-Trace)), TE=34.0/136.0/58.8ms, NEX=2/6/2, readout bandwidth=1796Hz/px, repetition time (TR)=8s, slice thickness=5mm, resolution=2.71×2.71mm^2, field-of-view (FOV)=26×19.5cm^2, partial Fourier factor =6/8. No parallel imaging was used. T_2-cDWI images were calculated using these data for each pairwise combination of b_c= 0, 750, 1500, 2250, 3000s/mm^2 and TE_c= 0, 75, 150, 225, 300ms, using in-house software [12]. The protocol was repeated such that T_2-cDWI difference images could be generated for each combination of b_c and TE_c. Regions-of-interest (ROIs), consisting of 75 pixels, were drawn within the vials on the images acquired at b=0s/mm^2 and TE=34ms, and then translated onto the difference maps. The variance of the difference values within these ROIs, divided by a factor of 2, provided an estimate for the true noise variance for T_2-cDWI. The estimated noise variance from equation 6 was computed and compared with the ground-truth values: σ^2 was estimated from values within the same ROIs placed on the difference map for the two images acquired at b=0s/mm^2 and TE=34ms.

Clinical Examples

To investigate the feasibility of T_2-cDWI in clinical settings, we applied T_2-cDWI prospectively to two patients on a 1.5T system (MAGNETOM Avanto, Siemens Healthcare, Erlangen, Germany). All the measurements were acquired with multiple averaging during free breathing using body-array surface receiver coils. The following cases were considered:

Patient 1: a 62-year-old male patient with malignant pleural mesothelioma (MPM). Combinations of b value and TE include (b = 100s/mm^2, TE = 82ms), (500, 82), (800,

82), (0, 60), (0, 82), and (0, 177). Other sequence parameters include: TR =8.1s, FOV=273×380mm^2, matrix = 128*92, 30 axial slices.

Patient 2: a 59-year-old female patient with ovarian cancer. Combinations of b value and TE include (b = 100s/mm^2, TE = 69.0ms), (600, 69.0), (1050, 69.0), (0, 26.4), (0, 102.0), and (0, 200.0). Other sequence parameters include: TR=5s, FOV=261×380mm^2, matrix = 160*110, 50 axial slices.

Computed images were generated for both clinical datasets using equation (3) at the following combinations of b_c and TE_c by using the same software [12]:

Patient 1: (b_c =1100s/mm^2, TE_c =82ms), (1100, 0), (0, 200).

Patient 2: (b_c =1200s/mm^2, TE_c =82ms), (1200, 0), (0, 300).

Results

Validation of T_2-cDWI model using a diffusion test-object

In Figure 3, it is observed that by synthesizing images at short echo times and high b-values it is possible to suppress the signal from components with long T_2 (vial 2, top-right image), whilst increasing the signal from components with low ADC but shorter T_2 (vial 5, top-right image, arrow). Direct acquisition of images with TE =0ms would not be possible. Conversely, by extending the TE_c to long values (e.g. 300ms) it is possible to increase the signal of regions with long T_2 (vials 2, bottom-left image) compared to other regions without requiring a significant increase in image acquisition time. Figure 2 demonstrates that true image noise in T_2-cDWI (black circles) is well approximated by equation (6) (surface plot) over the range of T_2, ADC, b_c, and TE_c values explored in this phantom. Furthermore, it is shown that the noise variance is lower than that expected by

direct calculation over the same image acquisition time (black wireframe) for many larger b/TE values.

Clinical Examples

In Patient 1 (mesothelioma), we observed two compartments within the disease (Figure 4 e&f): (i) solid tumour characterised by low ADC and short T_2 and (ii) pleural effusion with high ADC but long T_2. Both compartments were hyperintense on the acquired high b-value (Figure 4a) due to the T_2 shine-through effects caused by the long T_2 of pleural effusions. Although contrast improvements could be achieved by computing a higher b-value through conventional cDWI (Figure 4b), the suppression of T_2 shine-through was inadequate to discriminate between compartments. However, after decreasing TE_c to zero through the use of T_2-cDWI (Figure 4c), it was possible to reduce the hyperintense signal of pleural effusions, and improve the contrast of the solid tumour. Conversely, by using a high TE_c and low b_c (Figure 4d) it was possible to identify only those compartments associated with long T_2 and thus visualise the extent of pleural effusion.

Similar observations were made for Patient 2 (ovarian cancer). We identified a cystic region with high ADC and long T_2 that confounds the interpretation of the extent of solid disease on the native high-b-value DW image (Figure 5a). This remains confounding when a higher b-value was applied through the conventional cDWI (Figure 5b). By setting TE_c=0ms using T_2-cDWI, it was possible to eliminate the T_2 shine-through effects and improve the contrast between solid tumour and cystic components. Conversely, by setting b_c=0s/mm^2 and TE_c=300ms, we were able to enhance the signal from fluid and minimise signal from solid tumour to visualise the extent of the cystic region.

Discussion

We have developed a new acquisition and post-processing method that is able to reduce the T_2 shine-through effect that often confounds diffusion-weighted images, by allowing arbitrary modulation of T_2 and diffusion weighting. This is achieved by acquiring additional T_2-weighted EPI images at different echo times. Using the identical EPI readout ensures that the geometry- and B_0-related distortions are inherently matched. Through voxel-wise estimation of ADC and T_2 it is possible to synthesise image contrast corresponding to any combination of b-value and TE. It is important to note that the role of T_2-cDWI is purely a visualisation mechanism for improving image contrast for the identification of cellular tumours, and for separating confounding T_2 effects. We do not consider resulting images to be generally comparable with conventionally acquired images using the same b-value and echo time. In this context of visualisation, the diffusion model being used is not of primary concern provided that desirable tumour characteristic can be achieved. In this study, a joint monoexponential diffusion model was used without consideration of perfusion contribution, but the T_2-cDWI methodology easily lends itself to alternative diffusion models with appropriate data support.

We have derived analytical approximations to the noise characteristics of the T_2-cDWI model and validated the results through phantom experiments; in particular at high b-value and long TE combinations, T_2-cDWI images have reduced noise variance compared with acquired images. Increased signal noise was observed at low b-value and short TE combinations, due to the smaller number of signal averages at $b_c = 0 s/mm^2$, compared with a non-zero b-value, thus introducing larger errors [13].

Our clinical examples show T_2-cDWI was able to independently vary the image contrast by computation of images at desired b-values and echo times. With a large b-value and small/zero echo time, which are not possible to be acquired on the scanner, T_2-cDWI provided higher contrast for identifying areas of true impeded diffusion (e.g. tumour), due to efficient suppression of the T_2 shine-through effect, compared with acquired high-b-value images. Conversely, T_2-cDWI images with a low b-value and a long echo time enhance areas with long T_2 (e.g. fluid, effusion, and cystic disease) by effectively suppressing regions with shorter T_2. The greater freedom to adjust image contrast by manipulating b-values and echo times independently with T_2-cDWI may prove to be a useful clinical tool. There is a clear need for further investigation in future prospective studies, but our early proof of concept data appears promising. Other clinical uses of T_2-cDWI include multi-centre trials where computed TEs and b-values could be made equivalent for radiological reading thus minimising the impact of scanner variations in acquisition protocols. In addition, T_2-cDWI may facilitate automated segmentation based on the enhanced contrast.

Other authors have investigated the use of exponential images to eradicate T_2 shine-through effects by removing the S_0 component for conventional cDWI [14-16]. However, these images are associated with poor SNR and are not able to independently vary the relative contributions of both tissue diffusivity and T_2 relaxivity. Relaxation-corrected DWI [17] and short-TE cDWI [18] were used to correct for T_2 shine-through effect; however T_2-cDWI is able to provide synthetic images at any b-value and/or echo time. In another study, an ADC-dependent voxelwise cDWI (vcDWI) was proposed to improve

SNR and reduce T_2 shine-through effects [19], but without taking into account variations in tissue T_2-relaxation times.

In this study, the acquisition times for clinical studies were increased to acquire the additional T_2-weighted scans; however, the additional time was modest (<2 minutes for our example cases). In future studies, the dependence of image quality on the choice and number of echo times will be explored.

In this study, we were able to demonstrate objective and quantitative improvements in image noise and contrast when using the T_2-cDWI method.

Acknowledgement

This work is supported by CRUK and EPSRC Cancer Imaging Centre in association with the MRC and Department of Health grant C1060/A10334, C1060/A16464; NHS funding to the NIHR Biomedical Research Centre and post-doctoral fellowship funding by the NIHR (NHR011X); An Experimental Cancer Medicine Centre Network award (C51/A7401 & C12540/A15573) and British lung foundation (APP13-4). This paper presents independent research funded by the National Institute for Health Research (NIHR). The views expressed are those of the authors and not necessarily those of the NHS, the NIHR or the Department of Health.

References

1 Koh DM, Collins DJ (2007) Diffusion-weighted MRI in the body: applications and challenges in oncology. American Journal of Roentgenology 188:1622-1635

2 Koh DM, Takahara T, Imai Y, Collins DJ (2007) Practical aspects of assessing tumors using clinical diffusion-weighted imaging in the body. Magnetic Resonance in Medical Sciences 6:211-224

3 Malayeri AA, El Khouli RH, Zaheer A et al (2011) Principles and applications of diffusion-weighted imaging in cancer detection, staging, and treatment follow-up. Radiographics 31:1773-1791

4 Padhani AR, Liu G, Koh DM et al (2009) Diffusion-weighted magnetic resonance imaging as a cancer biomarker: consensus and recommendations. Neoplasia 11:102-125

5 Blackledge MD, Collins DJ, Tunariu N et al (2014) Assessment of treatment response by total tumor volume and global apparent diffusion coefficient using diffusion-weighted MRI in patients with metastatic bone disease: a feasibility study. PloS one 9:e91779

6 Blackledge MD, Leach MO, Collins DJ, Koh D-M (2011) Computed diffusion-weighted MR imaging may improve tumor detection. Radiology 261:573-581
7 Cheng L, Blackledge MD, Collins DJ, Tunariu N, Leach MO, Koh DM (2015) The use of Quantitative T2 to enhance Computed Diffusion Weighted Imaging. Intl. Soc. Mag. Reson. Med 23, Toronto, Canada, pp 3599
8 Bito Y, Hirata S, Yamamoto E (1995) Optimal gradient factors for ADC measurementsProc Intl Soc Magn Reson Med, pp 913
9 Jones D, Horsfield M, Simmons A (1999) Optimal strategies for measuring diffusion in anisotropic systems by magnetic resonance imaging. Magn Reson Med 42
10 Saritas EU, Lee JH, Nishimura DG (2011) SNR dependence of optimal parameters for apparent diffusion coefficient measurements. Medical Imaging, IEEE Transactions on 30:424-437
11 Kingsley PB (2006) Introduction to diffusion tensor imaging mathematics: Part II. Anisotropy, diffusion‐weighting factors, and gradient encoding schemes. Concepts in Magnetic Resonance Part A 28:123-154
12 Blackledge MD, Collins DJ, Koh D-M, Leach MO (2016) Rapid development of image analysis research tools: Bridging the gap between researcher and clinician with pyOsiriX. Computers in Biology and Medicine 69:203-212
13 Jones DK, Basser PJ (2004) “Squashing peanuts and smashing pumpkins”: How noise distorts diffusion‐weighted MR data. Magnetic Resonance in Medicine 52:979-993
14 Provenzale JM, Engelter ST, Petrella JR, Smith JS, MacFall JR (1999) Use of MR exponential diffusion-weighted images to eradicate T2 "shine-through" effect. American Journal of Roentgenology 172:537-539
15 Park SY, Kim CK, Park JJ, Park BK (2016) Exponential apparent diffusion coefficient in evaluating prostate cancer at 3 T: preliminary experience. The British journal of radiology 89:20150470
16 Tanimoto A, Nakashima J, Kohno H, Shinmoto H, Kuribayashi S (2007) Prostate cancer screening: The clinical value of diffusion-weighted imaging and dynamic MR imaging in combination with T2-weighted imaging. Journal of Magnetic Resonance Imaging 25:146-152
17 Chong DGQ (2013) Relaxation Corrected Diffusion Weighted Imaging. Intl. Soc. Mag. Reson. Med. 21, pp 3209
18 Kimura T, Sakashita N, Machii Y (2015) A short-TE Computed Diffusion Imaging (CDWI)Intl. Soc. Mag. Reson. Med 23, pp 2929
19 Gatidis S, Schmidt H, Martirosian P, Nikolaou K, Schwenzer NF (2015) Apparent diffusion coefficient‐dependent voxelwise computed diffusion‐weighted imaging: An approach for improving SNR and reducing T2 shine‐through effects. Journal of Magnetic Resonance Imaging

Legends:

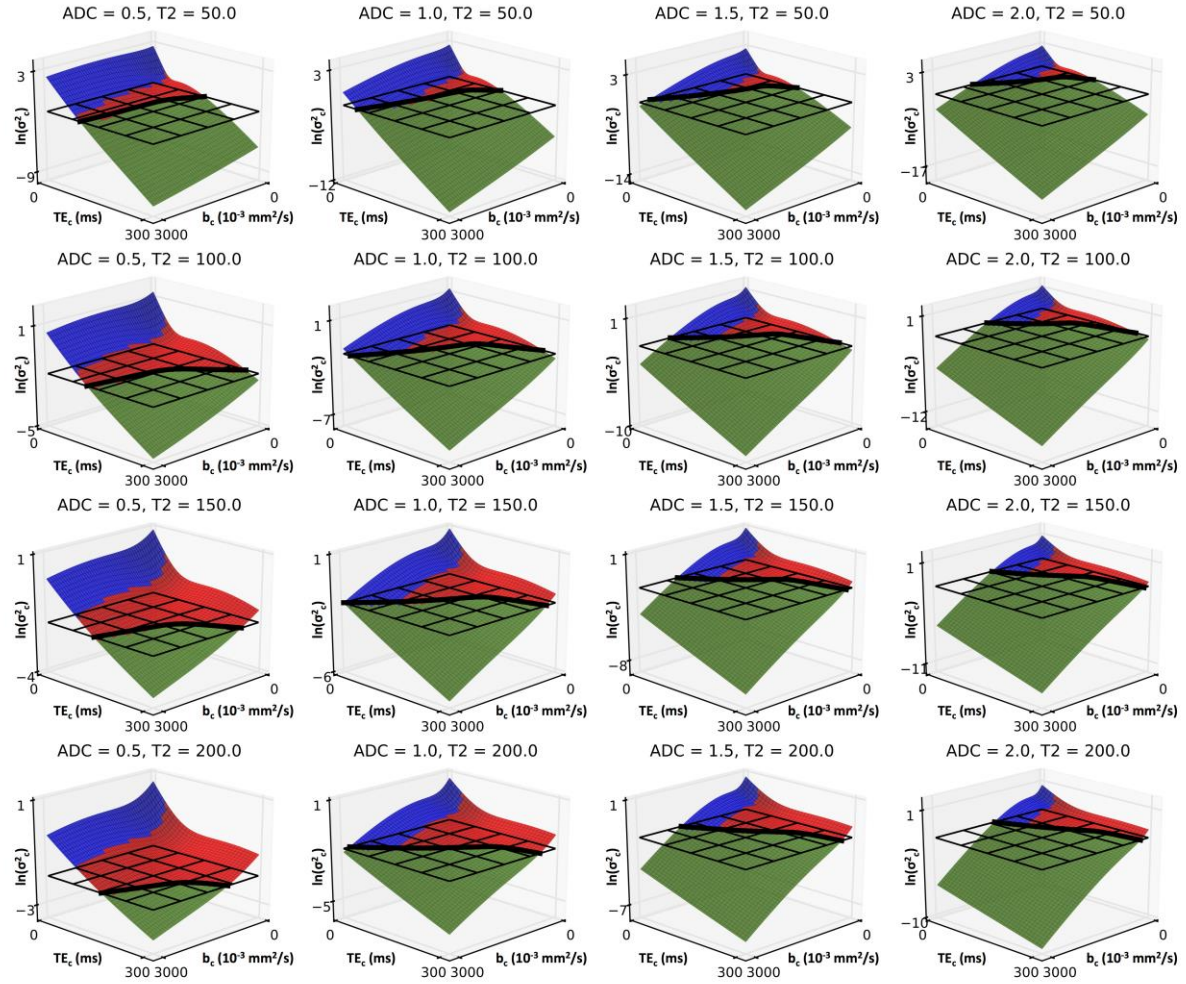

Figure 1: Comparison of the logarithm of noise variance from an optimally acquired T_2-cDWI sequence, $\sigma^2(b_c, TE_c)$ (surface-plot) with logarithm of noise-variance from a conventionally acquired sequence, $\sigma^2 = 1$ (black wireframe). Where $\sigma_c^2 < \sigma^2$, the surfaces are coloured in green. Areas in which the surfaces are coloured in blue represent those combinations of b and TE that could not be acquired directly using the given gradient performance of our scanner, otherwise they are coloured red. Units of ADC are given in $\times 10^{-3}$ mm^2/s, whilst for T_2 they are in ms. It is apparent there is often little advantage in directly acquiring images at a given b_c and TE_c combination (red surface areas) as T_2-

cDWI either affords improved SNR (green areas) or allows generation of images that would not be possible to acquire directly (blue areas).

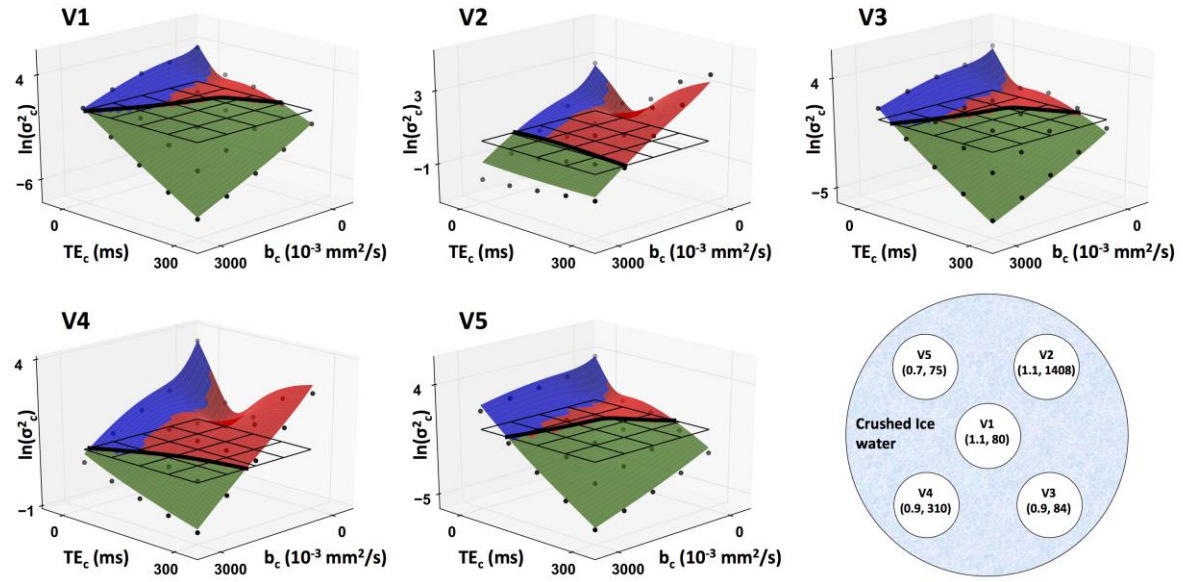

Figure 2: An illustration of the diffusion test-object is depicted in the bottom right. Each vial identifier is shown with its measured (ADC × 10^{-3} mm²/s, T_2 ms) values. Black circles in the surface plots represent measured noise variance, σ^2, for each of the vials in computed images with a range of b-values and echo times. The analytical estimation of the noise variance from the vial ADC and T_2 values is depicted as a surface plot (Green areas: $\sigma_c^2 < \sigma^2$, red areas: $\sigma_c^2 > \sigma^2$, blue areas: combinations of b and TE that could not be acquired directly using the given gradient performance of our scanner). There is a clear correspondence between the estimated and measured values for σ_c^2. Black wireframes indicate the expected noise variance for an acquisition scheme of equivalent acquisition time to T_2-cDWI, but with multiple image averages at each respective b_c/TE_c: The solid black line represents the intersection between the surface curves and the black

wireframes. It is observed that T_2-cDWI provides SNR advantages over conventional acquisitions for certain combinations of b_c/TE_c in this phantom.

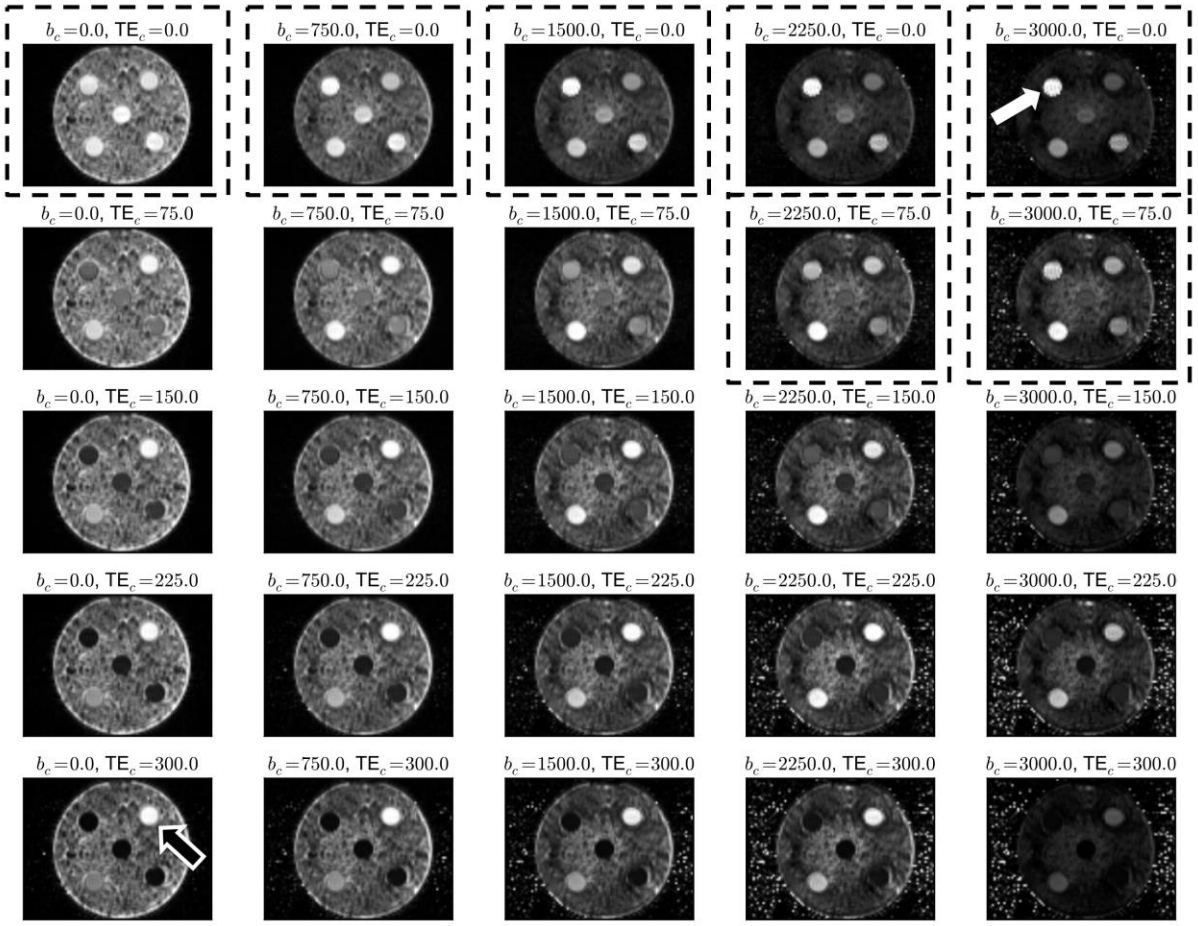

Figure 3: T_2-cDWI images of the diffusion test-object at varying computed b-values, b_c and echo times, TE_c. It is shown that by extrapolating the echo time to TE_c = 0.0 ms and the b-value to b_c = 3000 s/mm^2 it is possible to enhance the signal in the vial with low ADC and long T_2 (V5, white arrow). Conversely, by synthesising images with long TE_c we acquire images where the contrast favours components with a long T_2 (V2, black arrow). Those combinations of b_c and TE_c surrounded by black dashed boxes cannot be acquired directly using conventional diffusion-weighted EPI sequences. The windowing on all images has been set to optimise the visual contrast between vials.

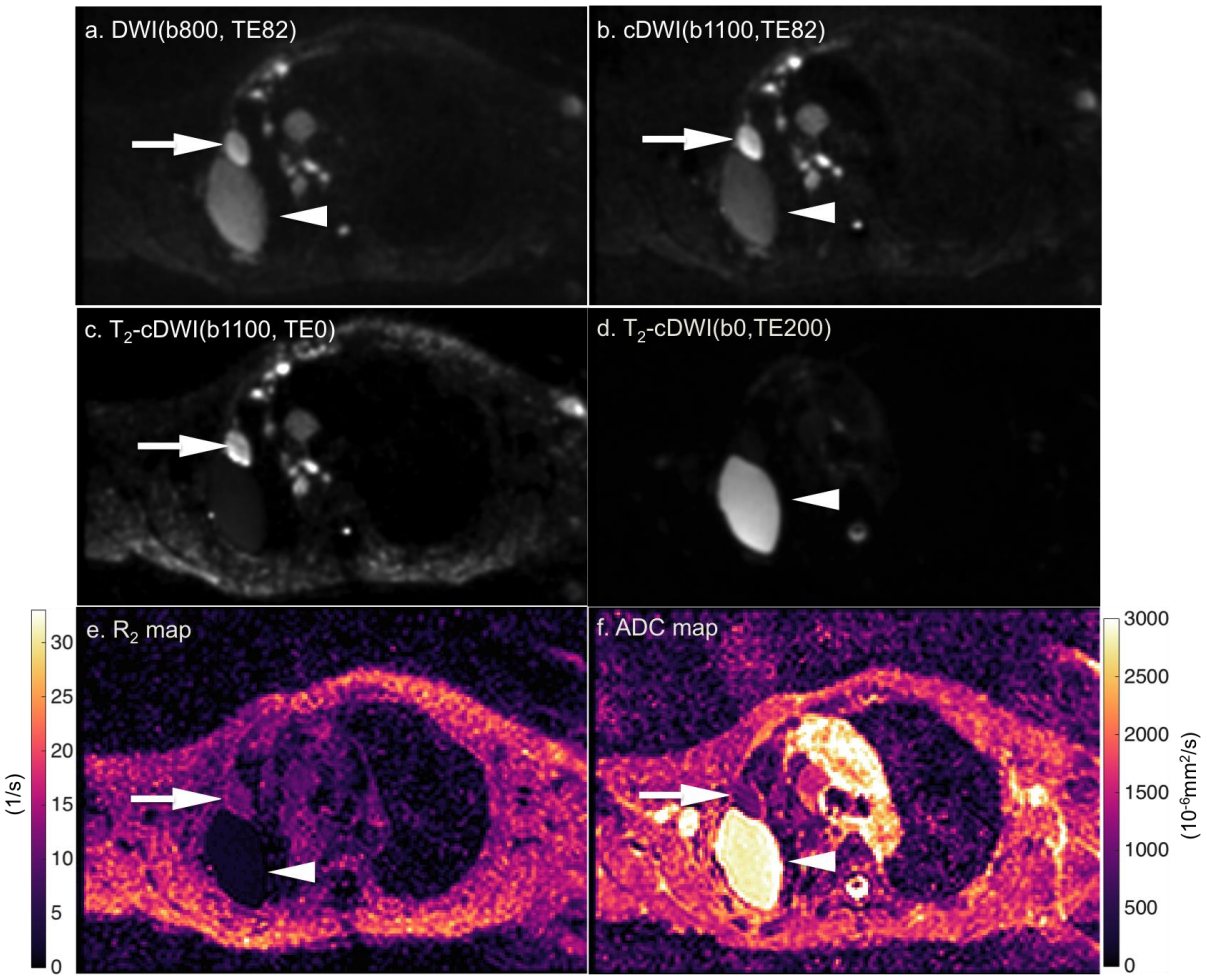

Figure 4: Axial DW MR images of a 62-year-old man with mesothelioma in the right lung for (a) acquired b-values of 800 s/mm^2 at TE of 82 ms, (b) computed b-value of 1100 s/mm^2 at TE of 82 ms, (c) T_2-adjusted computed b-value of 1100 s/mm^2, TE of 0 ms, and (d) T_2-adjusted computed b-value of 0 s/mm^2 TE of 200 ms. (e) R_2 map and (f) ADC map generated from all acquired images. The solid tumour (arrow) and pleural effusion (arrowhead) both show hyperintense signal on the acquired high-b-value DW image due to T_2 shine-through. Pleural effusions are still misinterpreted with solid disease even using a higher b-value in cDWI. By bringing the TE down to zero ms on T_2-cDWI, pleural effusions are suppressed very well and the solid tumour can be easily segmented out. In

contrast, using a very high TE and small b-value, the solid tumour and background tissue are suppressed. (For viewing of the colour R2 and ADC maps, the reader is referred to the online version of this article).

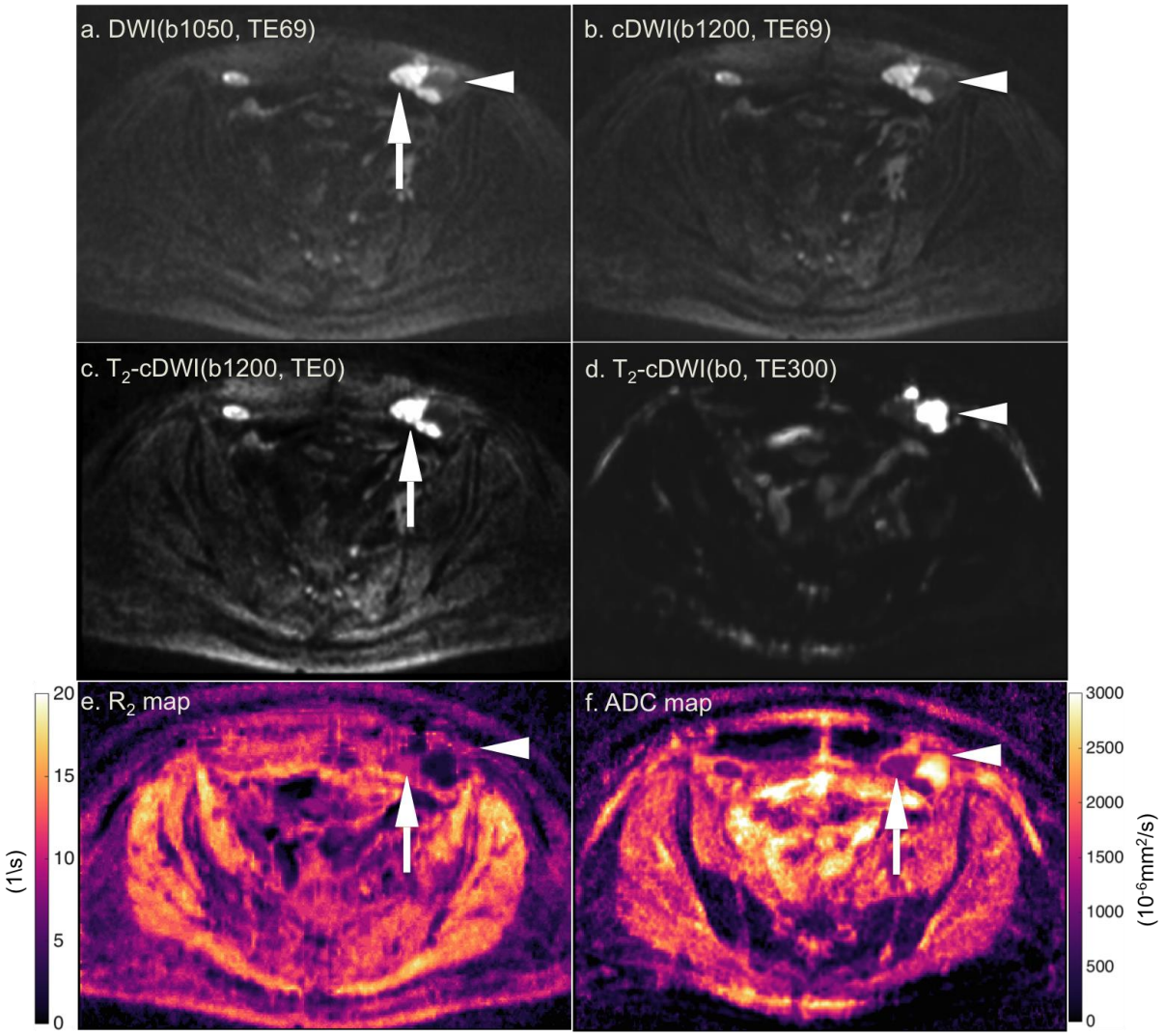

Figure 5: Axial DW MR images of a 59-year-old woman with ovarian cancer (a) acquired using b-values of 1050 s/mm^2 at TE of 69 ms, and (b) computed DWI (b-value of 1200 s/mm^2, TE of 69 ms), and (c) T_2-adjusted computed DWI (b-value of 1200 s/mm^2, TE of 0 ms). e) R_2 map and (f) ADC map generated from all acquired images. Arrow: ovary

tumour, arrowhead: cystic disease. (For viewing of the colour R2 and ADC maps, the reader is referred to the online version of this article).